PROCEEDINGS OF ECOS 2026 - THE 39TH INTERNATIONAL CONFERENCE ON

EFFICIENCY, COST, OPTIMIZATION, SIMULATION AND ENVIRONMENTAL IMPACT OF ENERGY SYSTEMS

28 JUNE – 03 JULY, 2026, CONSTANTA, ROMANIA

Optimization of a multi-service heat pump using natural and safe fluids and analysis of its seasonal performance

Ghady Zeghondy[a], Egoi Ortego Sampedro[b], Assaad Zoughaib[c], Karino Kang[d], Laura Nebot Andres[e], Rodrigo Llopis Domenech[f], Ramon Cabello Lopez[g], Alessandro Maccarini[h]

[a] *Ecole des Mines de Paris, Center for Energy, Environment, and Processes, 21 All. des Marronniers, 78000, Versailles, France, ghady.zeghondy@minesparis.psl.eu (CA)*

[b] *Ecole des Mines de Paris, Center for Energy, Environment, and Processes, 21 All. des Marronniers, 78000, Versailles, France, egoi.ortego@minesparis.psl.eu*

[c] *Ecole des Mines de Paris, Center for Energy, Environment, and Processes, 21 All. des Marronniers, 78000, Versailles, France, assaad.zoughaib@minesparis.psl.eu*

d Leviathan dynamics, 1 Centre Commercial de la Tour, 93120 La Courneuve, France., kkang@leviathan-dynamics.com

[e] *Miguel Hernández University of Elche, Avenida de la Universidad, 03202 Elche, Spain, lnebot@uji.es*

[f] *Jaume I University, Avinguda de Vicent Sos Baynat, 12071 Castelló de la Plana, Castellón, Spain, rllopis@uji.es*

[g] *Jaume I University, Avinguda de Vicent Sos Baynat, 12071 Castelló de la Plana, Castellón, Spain, cabello@emc.uji.es*

[h] *Aalborg University Copenhagen, A. C. Meyers Vænge 15, 2450 Copenhagen SV, Denmark, amac@build.aau.dk*

Abstract:

Recent regulatory changes restricting the use of hydrofluorocarbon (HFC) refrigerants have significantly affected heat pump technologies, as these systems have traditionally relied on them. At the same time, European regulations targeting per- and polyfluoroalkyl substances (PFAS), commonly referred to as "forever chemicals," are becoming increasingly stringent. Hydrofluoroolefin (HFO) refrigerants have emerged as potential alternatives; however, their decomposition may generate PFAS, raising concerns about future regulatory limitations. Other options, such as hydrocarbons, present flammability risks, while natural refrigerants like water offer environmental and safety advantages. Nevertheless, the use of water in air-to-water heat pumps is constrained by its triple point temperature. To address these challenges, recent research has focused on an innovative cascade system combining water and CO_2 to overcome such limitations. This study investigates the feasibility of integrating a water–CO_2 cascade heat pump system to meet residential heating and domestic hot water (DHW) demands throughout the year. An optimization of operating conditions is carried out to adjust system pressures and temperatures according to ambient conditions and heating requirements. Two heating regimes are considered, corresponding to low- and medium-temperature emitters governed by weather compensation laws. Additionally, different operating modes are analyzed to determine the most efficient configuration for each time step, ensuring demand coverage while maximizing performance. A simplified linear model is used to estimate the heating load. The optimized cascade performance is then used to evaluate the seasonal coefficient of performance (SCOP) under varying climatic conditions across different countries. Finally, the proposed system is compared with a conventional propane-based heat pump. The results show that the cascade system performs better under high-temperature heating regimes (47–55°C), while it is slightly less efficient under low-temperature regimes (30–35°C).

Keywords:

Heat pump, regulations, risks, temperature, heating, domestic hot water, optimization, working conditions, cascade, weather compensation laws, seasonal coefficient of performance.

1.Introduction

Since the Industrial Revolution, greenhouse gas (GHG) concentrations have increased significantly worldwide. This rise, driven by sectors such as industry, transportation, agriculture, and energy, has led to major environmental impacts, including a 1.1°C increase in global temperature, extreme weather events, species extinction, polar ice melting, ozone layer depletion, increased ultraviolet radiation exposure, and related health issues due to higher pollutant concentrations[1].

The industrial and household sectors are among the main contributors due to their high-energy demand, largely dependent on fossil fuels. In the European Union, industry accounts for about 26% of total final energy use, with 66% dedicated to heating processes[2](Figure 1). Meanwhile, households consume about 28% of total energy[3], largely for space heating and domestic hot water (Figure 1). The reliance on traditional sources, such as gas and oil, leads to substantial emissions. For example, heating accounts for nearly 70% of residential energy use in Germany and the USA[1-4], and 80% of households in the UK still use gas boilers [2]. These statistics highlight the urgent need for more sustainable energy solutions across both sectors.

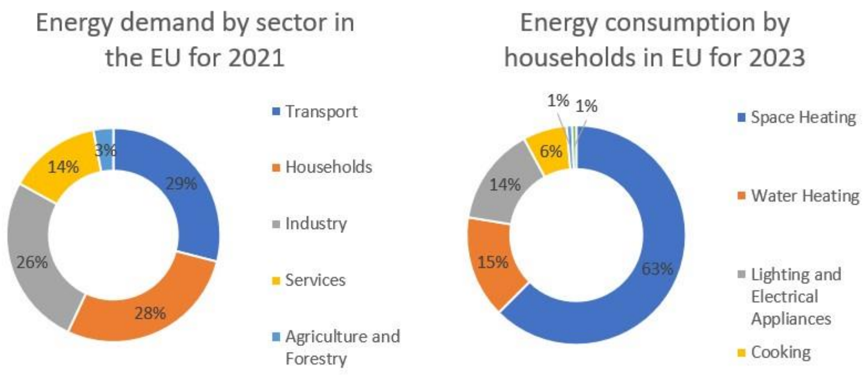

Figure 1. *Energy consumption in the EU, divided by sector for the year 2021 and by household for the year 2023.*

Given the significant impact of GHG emissions, countries, particularly in Europe, are implementing strategies to reduce them. The European Union, through Regulation No. 517/2014, aims to cut emissions by 80–90% by 2050 compared to 1990 levels. In this context, heat pumps are increasingly adopted, as they use waste [5] or atmospheric[6] heat to provide heating, cooling, and domestic hot water [7], [8]. In fact, their installations have increased from 35% to 38% in the EU in 2022, as stated by the International Energy Agency (IEA)[9]

However, current progress remains insufficient, leading to stricter regulations on high global warming potential (GWP) refrigerants such as hydrofluorocarbons (HFCs). Denmark, Germany, the Netherlands, Norway, and Sweden have proposed restrictions on PFAS, including HFO/HCFO working fluids, under REACH due to their toxicity and flammability [10]. Additionally, commonly used refrigerants like propane, R-410A, and R134a are being phased out due to safety concerns or high GWP.

As a result, the heat pump industry is shifting toward more environmentally friendly alternatives. Water and CO_2 are emerging as promising solutions due to their low environmental impact, non-toxicity, and non-flammability, while maintaining good performance. In case of leakage or accidental release, neither poses any significant safety or environmental risk [10].

While these refrigerants have a lower environmental impact, their application is limited by performance constraints related to their physical properties, making them less suitable for certain applications.

CO_2 heat pumps operate in subcritical or supercritical modes, constrained by a low critical temperature (31°C) [11]. Subcritical Systems, operating below critical temperature, showed a higher coefficient of performance (COP) than supercritical ones due to lower compression work [12], but cannot reach high temperatures, necessitating a shift to supercritical modes. Supercritical CO_2 systems require components that can sustain very high pressures [13], which contributes significantly to system cost and energy consumption. Also, despite the widespread use of this system for water heating, due to having a heat exchange temperature profile curve close to the water temperature profile curve, resulting in a lower pinch, with a better performance if the water inlet temperature is low[12-14]; this regime did not perform well for space heating [15].

Water is a very promising refrigerant due to its environmental friendliness and excellent thermophysical properties [16], and new compressor technologies are being developed worldwide, such as by Leviathan Dynamics and Alpinov X in France. Its high latent heat of vaporization allows more heat absorption with less circulated mass, reducing the required fluid quantity. In addition, water heat pumps can achieve high COPs (3–4) depending on the configuration, reach temperatures up to 100°C, and are of interest to many industry players, as simple vapor compression cycles are the most widely used [17]. However, water heat pumps have limitations. Household-relevant operation requires vacuum pressures, complicating leak control and maintenance [18]. Additionally, water vapor's low density demands high volumetric flow rates and thus large compressors, increasing system cost and installation space. Moreover, water freezes below 0°C, restricting the operating range.

To offer a heat pump that uses non-dangerous natural fluids for cold climates, this article explores the operating principles of a new heat pump solution based on a water-CO_2 cascade for the production of heating and domestic hot water.

Thermodynamic cascades are well known. In cascaded systems, each cycle handles a part of the heating load within its temperature range, covering a wider range of operating conditions and applications[17]. By combining CO_2 for the low-temperature range and water for the high-temperature range, cascaded systems overcome the temperature limitations of each fluid and achieve a larger overall range. Cascaded heat pumps generally offer better performance than single-stage systems. Dai et al. (2022)[19] reported that high-temperature cascade heat pumps (e.g., CWSAS configuration) reduce primary energy consumption by 1.8–22.8% compared with conventional high-temperature heat pumps, and by 3.4–19.2% compared with electric boilers. This results in reduced consumption and emissions, contributing to worldwide energy objectives. Also, lifecycle carbon emissions of cascaded cycles are claimed to be reduced by 1.7–6.1% when compared to conventional systems, and by 76.5% when compared to electric boilers[19].

The envisioned system consists of two cascaded cycles: a carbon dioxide (CO_2) cycle as the low-temperature cycle and a water cycle as the high-temperature cycle. Figure 2 shows the cascade component arrangement.

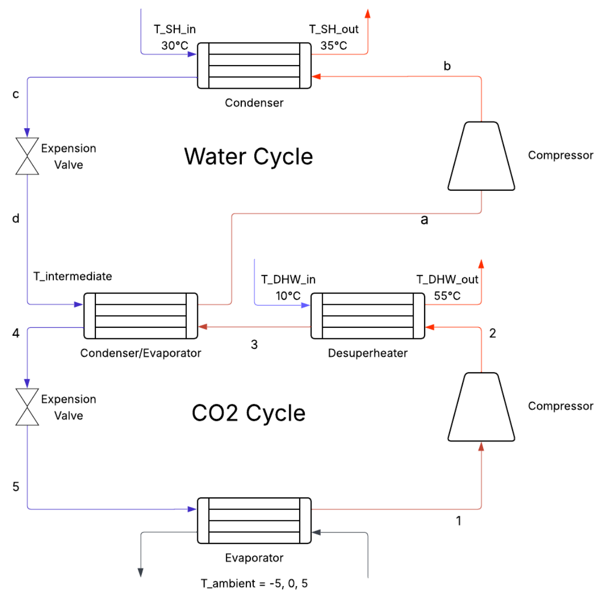

Figure 2. *The cascade system used and the component arrangement*.

The CO_2 cycle functions by extracting heat from the atmosphere for space heating and/or domestic hot water production (DHW). DHW is achieved through a desuperheater, a heat exchanger placed between the compressor and condenser of the same cycle that utilizes only the superheated portion of the CO_2 cycle. The remaining heat is then transferred to the water cycle, which raises the temperature and delivers it to the space or DHW system, depending on the operating mode.

This configuration overcomes the limitations of each refrigerant and allows operation over a wider combined temperature range. Since water cannot operate below 0°C, CO_2 serves as the lower cycle, enabling heat extraction even in winter at low ambient temperatures. Conversely, due to CO_2's low critical temperature and COP deterioration above this point, water is used as the upper cycle, capable of reaching higher temperatures in its subcritical regime.

The objective of this paper is to determine the system's optimal operating conditions across different modes (heating, DHW, and mixed). The optimization method is presented, followed by an annual performance assessment using simplified load models and weather-compensated low- and medium-temperature emitters.

2. Operating conditions and modeling framework

For residential applications, three operating modes are defined. Full heating mode occurs when only space heating is required, typically during winter nights. Full domestic hot water (DHW) mode is used when space heating is unnecessary, mainly in summer. Mixed mode provides both space heating and DHW simultaneously. The system configuration remains largely unchanged across modes; only the inlet and outlet temperatures of the external water cycles vary according to the selected mode.

2.1. Load calculation

The system is sized for a reference 150 m² house in Denmark meeting the KFW 55 standard, with annual energy consumption of 18 kWh/m² for domestic hot water and 35 kWh/m² for space heating, used to calculate the design power[20]. Since the DHW load varies with occupancy and ambient temperature, a normalized hourly energy usage profile is employed (Figure 3)[20].

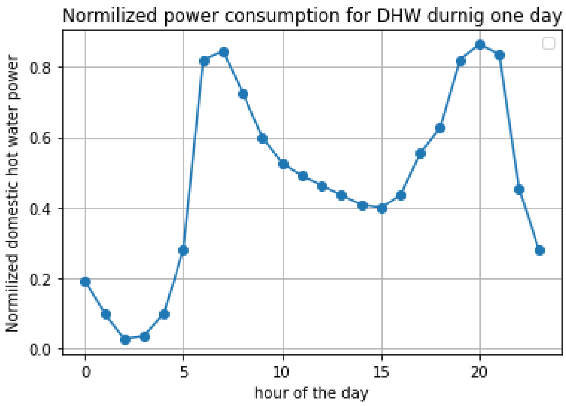

***Figure 3**. Figure of the normalized domestic hot water power in residential buildings.*

To better assess system performance, the seasonal coefficient of performance (SCOP) is used, providing results that more closely reflect real operating conditions. SCOP depends on several factors, first, the load model, which can be approximated as a linear function of the form:

$$\dot{Q}_{load}(T_{amb}) = \dot{Q}_{design}\left(1 - \frac{T_{amb} - T_{design}}{T_{0\_load} - T_{design}}\right) \quad (1)$$

The zero load temperature (T_{0_load}) is set to 16°C for this study, above which only domestic hot water is provided. For very low consumption buildings, it can be lower[21]. The design temperature (T_{design}) depends on the climatic area and varies according to Table 1. While the standard provides guidance, the choice must also consider technical and economic factors such as weather conditions and installation costs. For simplicity, a value of –10 °C is used, consistent with the weather data applied.

***Table 1**. T_{design} as a function of the type of weather (EN14825).*

	Cold	Average	Warm
$\boldsymbol{T_{design}(°C)}$	-22	-10	2

The design load depends on the case studied and is chosen so that the annual heating energy consumption equals 35 kWh/m². The heat pump capacity variation model describes the percentage of heat pump power used, which decreases with ambient temperature due to reduced pressure and vapor density at the compressor inlet. The bivalent temperature (T_{biv}) is the temperature at which the heat pump output will exactly meet the load. Above this value, an additional heat source will be required, such as an electric resistance or a gas boiler. The reduction factor RF is defined as the ratio of the heat pump's bivalent capacity $\dot{Q}_{heat_{HP}}(T_{biv})$ to its capacity at other ambient temperatures, $\dot{Q}_{heat_{HP}}(T_{amb})$:

$$RF(T_{amb}) = \frac{\dot{Q}_{heat_{HP}}(T_{amb})}{\dot{Q}_{heat_{HP}}(T_{biv})} \tag{2}$$

In addition, with dh_{ev} the evaporation enthalpy, ρ_{ev} the vapor density at compressor inlet, and $\dot{V}$ the swept volume, and the volumetric efficiency η_{vol} is assumed to be 1, the capacity ratio can be written like this:

$$RF(T_{amb}) = \frac{dh_{ev}(T_{amb})\rho_{ev}(T_{amb})\,\dot{V}\,COP(T_{amb})/\,(COP(T_{amb}) - 1)}{dh_{ev}(T_{biv})\rho_{ev}(T_{biv})\,\dot{V}\,COP(T_{biv})/(COP(T_{biv}) - 1)} \tag{3}$$

The swept volume is considered constant at temperatures below $T_{biv,}$ so it is simplified in the above equation. The capacity ratio is only applied to ambient temperatures below T_{biv}. For this work $T_{biv} = T_{design}$.

Lastly, the weather compensation laws help in reducing the energy consumption of the heat pump and improving comfort through adapting the heating of the return water temperature to the ambient temperature. This concept also depends on the type of heat emitter installed.

A classical way of defining a weather compensation law for the return water temperature ($T_{w\,r}$) is using the following relation:

$$T_{w\,r} = T_A + k\,(T_{room} - T_{amb}) \tag{4}$$

With:

k: Slope depending on the type of emitter taken to be 0.5 for floor heating and 0.95 for low/medium emitters, according to the "Atlantic" heat pump manufacturer.

T_{room} : Desired indoor temperature in °C.

T_A : Offset temperature in °C. It can be equal to T_{room} in some controllers.

T_{amb} : Weather-dependent temperature in °C.

2.2. Parameters and variables

The system is optimized by adjusting key parameters, constraints, and variables. The ambient temperature, representing the weather conditions, was considered using one year of Helsinki data for efficiency, although variations over five years in Milan, Paris, Copenhagen, Madrid, and Helsinki were available (Figure 4). Ambient temperature affects the CO_2 evaporating temperature, which must satisfy a minimum pinch constraint of 3° in the desuperheater and water condenser. For the pinch in the intermediate heat exchanger, it is fixed at a value of 3°, since the condensing temperature of CO_2 is found using the intermediate temperature ($T_{cond_{CO_2}} = T_{inter} + pinch$). The return temperature of the external water cycle, which varies with ambient temperature, influences the condensing temperature of water, and adjusting the intermediate temperature ensures that the pinch point constraint is met. Subcooling and superheating were applied at 0 °C for both refrigerants and 10 °C for CO_2, respectively. Finally, the CO_2 compressor efficiency from Nebot-Andrés et al. (2017) [22] was used, expressed as a function of the pressure ratio between the compressor inlet and outlet (equation 5).

$$\eta_{comp_{CO_2}} = A - B\left(\frac{P_{cond_{CO2}}}{P_{evap_{CO2}}}\right) \qquad where\ A = 0.7359, \quad B = 0.0517 \tag{5}$$

In addition to the parameters, a set of variables is specified and iterated to find the optimum combination leading to maximizing the COP and SCOP. The first variable is the intermediate temperature, which is the evaporating temperature of the water cycle and is related to the condensing temperature of CO_2 through the pinch ($T_{cond_{CO_2}} = T_{inter} + pinch = T_{evap_{water}} + pinch$). It varies from 1°C to 26°Censuring compatibility with both refrigerants. The second variable is the margin temperature defined as the temperature difference between the outlet temperature of the desuperheater and the saturated temperature of the desuperheater ($\Delta T_{desuperheater} = T_{desuperheater_{out}} - T_{cond_{CO_2}}$). This temperature difference ensures that the pinch requirement is met whenever the intermediate temperature is low and cannot satisfy it alone, or whenever the external inlet cold liquid water temperature exceeds the intermediate temperature's upper limit. In such cases, the margin temperature intervenes to stop desuperheating at the point where the pinch is minimal but still satisfied. The following figure, Figure 5, shows the location of the parameters and variables on the TS diagram of the system.

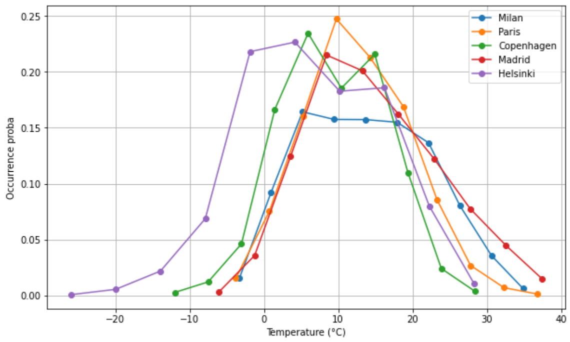

***Figure 4.** Ambient temperature variation of Milan, Paris, Copenhagen, Madrid, and Helsinki.*

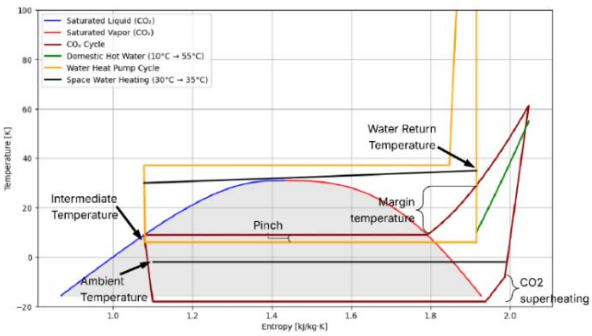

***Figure 5**. Cycle's TS- diagram showing the parameters and variables locations.*

2.3. Methodology of the work

After defining all parameters and variables to determine the optimal operating conditions for each mode and maximize the overall COP at each ambient temperature, a Python code was developed using the necessary libraries. CoolProp was used to calculate thermodynamic states at all cycle points, while scipy.optimize provided the optimization tools. First, the "minimize" function optimized pressures in the heat exchangers to satisfy pinch requirements, effectively handling this local optimization problem. Then, the differential evolution algorithm explored variable combinations systematically to identify the global optimum configuration, generating new candidate solutions via weighted combinations of previous ones, while handling constraints such as heat exchanger pinch conditions. However, no technological constraints, such as compressor compression ratio limits, were considered in this study. Furthermore, due to weather compensation laws, when the ambient temperature exceeds 16°C, space heating is stopped, and the system operates exclusively in domestic hot water production mode if needed.

During execution, the code calculates the system state points, evaluates the achievable overall COP under all constraints, identifies and stores the optimal parameter set for each ambient temperature, and ultimately computes the seasonal COP (SCOP) of the system.

$$COP_{CO2} = \frac{\dot{Q}_{desuperheater_{CO2}} + \dot{Q}_{condenser_{CO2}}}{\dot{W}_{comp_{CO2}}} \quad (6)$$

$$COP_{Water} = \frac{\dot{Q}_{cond_{water}}}{\dot{W}_{comp_{water}}} \quad (7)$$

$$COP_{total} = \frac{\dot{Q}_{desuperheater_{CO2}} + \dot{Q}_{cond_{water}}}{\dot{W}_{comp_{CO2}} + \dot{W}_{comp_{water}}} \quad (8)$$

$$SCOP = \frac{\dot{Q}_{hot_{yearly}}}{W_{electric_{yearly}}} \quad (9)$$

After determining the optimal solutions, the system is sized to provide a total annual heating load of 5250 kWh/year (35 kWh/m² × 150 m²), based on a design temperature that allows the system to meet the load with desirable performance throughout the year.

Then, using the hourly average ambient temperature in Helsinki for one year, the hourly loads for domestic hot water (DHW) and space heating are calculated. From these loads, the ratio of DHW power to the required heating load is determined, guiding the operating mode: a ratio of zero corresponds to full heating mode, a ratio of one to full DHW mode, and intermediate values trigger a mixed regime. In some cases, the system may operate fully in one mode initially and then switch to the second mode to meet the remaining load. Furthermore, if the ratio closely matches the optimal power division at a given ambient temperature, the system remains in mixed mode for the entire period. However, if the ratio does not match the optimal power division and is closer to zero, it starts in mixed mode and transitions to full heating, whereas if it is closer to one, it transitions from mixed mode to full DHW operation.

3. Results and discussion

The results of this study show how each variable and parameter affects the behavior of the system, providing a better understanding of its performance under different weather and operating conditions. Therefore, it is necessary to study each factor individually to understand its behavior and variation with respect to the input parameters. All operating modes and heating regimes exhibit the same overall trends in response to changes in variables and parameters, although the magnitude of these changes may differ.

3.1. Effect of the ambient, intermediate, and margin temperatures on the COP

Since the ambient temperature positively affects the evaporating temperature of the CO_2 cycle, it has a positive relationship with the CO_2 cycle and overall COP. As the ambient temperature increases, the evaporating temperature of CO_2 increases to satisfy the minimum pinch of 3°, reducing the pressure difference across the compressor. This lowers its work and increases both the cycle and overall COP. This is shown by the difference in COP results (black solid curve) between a system operating at -5°C, achieving a highest COP of 3.4 (Figure 6.a), and one at 5°C, achieving 4.1 (Figure 6.b). However, this increase also decreases the compressor outlet temperature, which must be monitored to ensure sufficient heat transfer in the desuperheater.

In contrast, the intermediate temperature affects both cycles and the overall performance. As it increases, the condensing temperature of the CO_2 cycle increases, shifting the constant condensing pressure line upwards. This increases the pressure difference across the compressor and reduces the COP of the lower cycle. For the water cycle, however, this temperature acts as the evaporating temperature and has a similar effect to ambient temperature on the CO_2 cycle. As it increases, the pressure difference across the water compressor decreases, increasing its COP. Since this temperature has opposite effects on each cycle, and because the overall COP follows the CO_2 cycle behavior, the CO_2 cycle dominates system performance.

On the other hand, the margin temperature ensures that the pinch requirement is met at low intermediate temperatures or high operating regimes by complementing the intermediate temperature. This is shown in Figure 6.a, where at an intermediate temperature of 5°C and ambient temperature of -5°C, a margin temperature of 0° (red solid curve) fails to satisfy the pinch constraint (dashed horizontal grey line), whereas a 10° margin temperature (red dashed curve), for the same intermediate and ambient temperatures, achieves it, extending the feasible operating range. However, using a higher margin temperature reduces performance by restricting the desuperheater power through increasing its outlet temperature, as shown by the difference between the black solid and dashed curves in Figure 6.

In conclusion, while ambient temperature positively influences COP, intermediate and margin temperatures negatively affect it; hence, their careful combination is essential to satisfy system constraints and balance performance with feasibility.

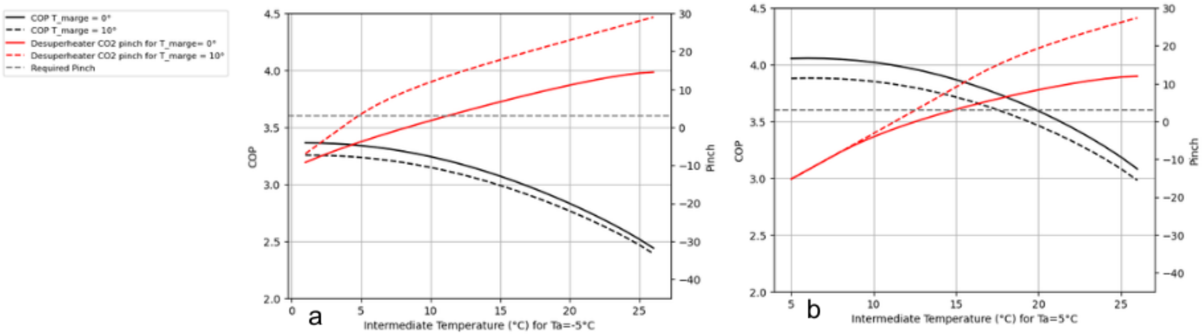

Figure 6. *The effect of intermediate and ambient temperature on the overall COP of the system.*

3.2. Optimal results for different operating modes and heating regimes

In addition, system performance is influenced by the operating modes and heating regimes. Changing either alters the cold liquid water inlet temperature to 10°C for domestic hot water, or 30°C or 47°C for space heating, requiring a change in the intermediate and margin temperature combination to satisfy the pinch requirement. These changes affect the operating pressures and therefore vary the compressor work, influencing system performance. Moving from full domestic hot water mode to full space heating, or from a low heating regime to a higher one, requires a higher combination of intermediate and margin temperatures to satisfy the pinch due to the low critical temperature of CO_2, which deteriorates the COP, as explained in section 3.1. However, the results show otherwise. A full heating mode at 30/35°C is more efficient than a full domestic hot water mode at 10/55°C (Table 2). This is because the domestic hot water mode has a steeper temperature slope, requiring a higher condensing temperature in the water cycle, reflected in a higher compression ratio and increased compression work, thus decreasing the COP.

Furthermore, the mixed mode is the most beneficial operating mode, as shown by the comparison in Table 2, and should be used whenever both loads are required. If both loads are needed and their distribution matches the optimal power ratio, the system should operate continuously in mixed mode. Otherwise, the system first operates in mixed mode and then switches to another mode to meet the remaining demand. For example, at an ambient temperature of 10°C, the optimal power ratio is 0.5 of domestic hot water to heating power (Table 2) for a 30–35°C regime, while the required ratio is 0.17 (approximately yearly hours 2500, Figure 7.a). Therefore, the system operates in mixed mode first to cover the domestic hot water demand and part of the heating load, then switches to full heating mode, after covering the domestic hot water load, to cover the remaining heating load (Figure 7.d).

Table 2. *The variation of the coefficient of performance and the water compression ratio with the operating mode and heating regime.*

Ambient temperature	**Full DHW (10-55°C)**		**Full heating (30-35°C)**		**Full heating (47-55°C)**		**Heating (30-35°C) + DHW (10-55°C)**			**Heating (47-55°C) + DHW (10-55°C)**		
	COP	τ_{water}	COP	τ_{water}	COP	τ_{water}	COP	τ_{water}	Optimal Load Ratio	COP	τ_{water}	Optimal Load Ratio
-5	2.9	11.1	3.1	7.3	2.5	14.3	3.3	6.6	0.3	2.7	13.1	0.4
0	3.1	9.1	3.4	6.1	2.6	11.9	3.6	5.2	0.3	2.9	11.5	0.4
5	3.3	7.6	3.7	5.7	2.8	10.1	3.9	4.1	0.4	3.1	9.9	0.4
10	3.6	6.4	4.1	4.4	3.0	8.7	4.3	3.2	0.5	3.4	8.5	0.4
15	3.9	5.5	4.7	4.1	3.2	7.0	4.7	2.7	0.5	3.7	7.1	0.5

3.3. Optimal results for yearly analysis

After analyzing the weather data for the city of Helsinki, the system was designed and sized to deliver a capacity of 1600 W at a design temperature of −10 °C. This sizing ensures that the system can adequately meet the residents' heating demand throughout the year, with an SCOP of 3.64, reflecting operation under realistic conditions, which also influences the return water temperature for heating. As the ambient temperature increases, the return water temperature decreases, leading to a reduction in heat supply until the system stops operating for space heating at an ambient temperature of 16 °C and above.

To calculate the SCOP of the system, a detailed analysis was performed on the hourly energy demand and the operating modes to ensure accurate load coverage under optimal performance. First, the optimal COP of each operating mode at different ambient temperatures was determined. Then, using the hourly ambient temperature shown in Figure 7.a, the hourly heating load throughout the year was calculated, as illustrated in Figure 7.b. For the DHW, an hourly load distribution, demonstrated in Figure 7.c, was used, obtained from a total daily amount of 7.4 kWh and the normalized daily distribution in Figure 3. This load is assumed to be the same for all days of the year.

From this information, an analysis of the operating mode to be adopted, or the alternation between modes, was carried out in order to operate the system at the highest performance while meeting the required load. As expected, and as shown in Section 3.2, the system operates predominantly in mixed mode due to its higher performance, as seen in Figure 7.d, which shows the operating mode load coverage percentage required hourly to accurately cover the system load.

Finally, the power required from the system to cover the yearly load was determined based on the operating mode adopted and its optimal COP, as well as the functioning time of the mode. The SCOP was then calculated from the total yearly heat provided and the total electrical energy consumed.

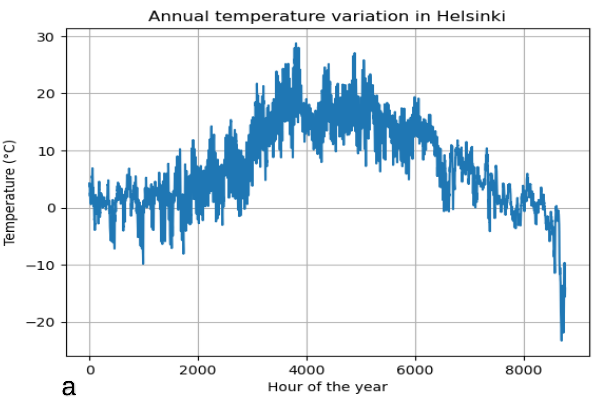

a

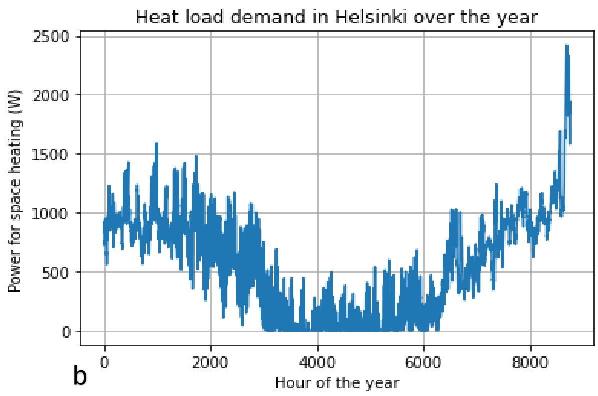

b

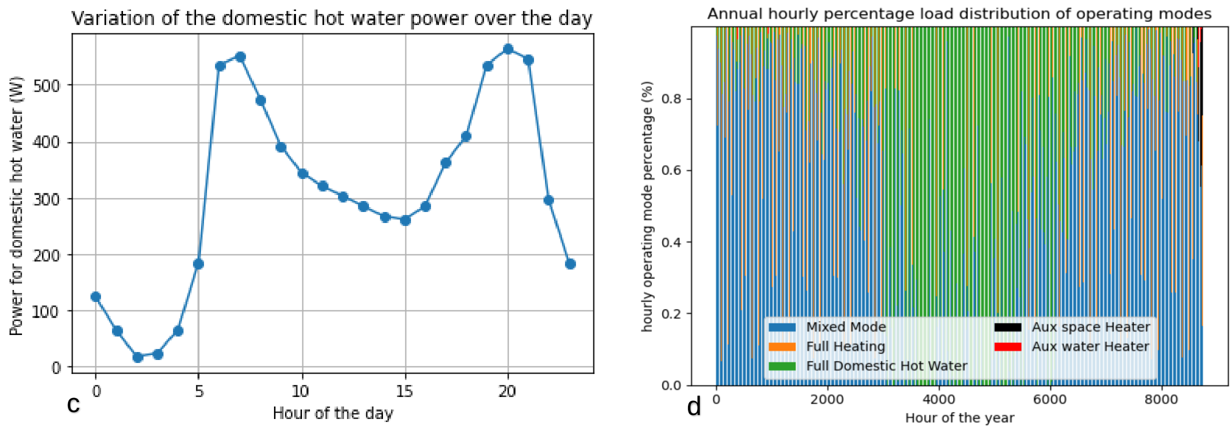

Figure 7*.* *The variation of temperatures and heat loads over the days and years*.

3.4. Comparison with a propane heat pump

To evaluate the performance of the proposed system, a comparison was conducted with a conventional propane heat pump.

Table 3. *Comparing the performance of the envisioned system versus the propane one*.

Ambient Temperature (°C)	**Coefficient of Performance**			
	Propane full heating		Cascade full heating	
	30-35°C heating regime	47-55°C heating regime	30-35°C heating regime	47-55°C heating regime
-5	3.1	2.3	3.1	2.5
0	3.4	2.5	3.4	2.6
5	3.8	2.7	3.7	2.8
10	4.3	2.9	4.1	3.0
15	4.9	3.1	4.7	3.2

On the one hand, the suggested system performs better under high-temperature heating regimes than the propane-based system for fixed heating regimes, but shows lower performance at lower temperatures. According to Table 3, the suggested system achieves a COP of 3 for a full heating mode with a heating regime of 47–55°C and an ambient temperature of 10°C, which is almost 3.5% better than the propane cycle's 2.9. However, at a low heating regime of 30-35°C, the propane system achieves a COP value of 4.3, which is 5% higher than the proposed system's COP value of 4.1 for the same ambient temperature.

Table 4. *Comparison of the SCOP for both systems for different Kc values*

Kc	**Seasonal Coefficient of Performance SCOP**	
	Cascade Cycle	Propane Cycle
0.5	4	3.76
0.95	3.63	3.43

On the other hand, the propane system is less efficient than the cascade system in terms of power consumption and SCOP when weather compensation laws are taken into account. For the two cases of Kc studied in this research, the SCOP of the propane cycle is 6% lower than that of the cascade cycle as can be seen from Table 4. Since both systems are exposed to the same load, the difference in SCOP can be mainly attributed to the lower compressor power consumption in the cascade system, which results from its more favorable thermodynamic operating conditions.

In addition to demonstrating a marginally better performance regarding the SCOP, the proposed cascade system offers also significant advantages in terms of environmental impact and long-term sustainability, as it relies on working fluids with lower environmental impact and presents improved safety characteristics compared to propane-based systems. Besides, further architecture optimization studies will be performed on the cascade in order to improve the full-DHW mode.

4. Conclusion

This study demonstrates the technical viability of the suggested system for residential use because it effectively satisfies the yearly heating demand in spite of temperature variations. The system, designed for a load of 1600 W at −10°C, is able to satisfy the total heating demand of the residential unit during the year.

Additionally, the system can adjust to the various thermal requirements through the implementation of three operating modes, guaranteeing optimal performance under various conditions. When space heating and hot water production are required, the mixed mode is adopted as it provides the best performance. However, the operational constraint that restricts heating modes and regimes at ambient temperatures above 16°C plays an important role in the overall performance of the system as it imposes the use of the full domestic hot water mode.

Furthermore, the analysis shows that the operating temperatures have a major impact on the system's performance. Specifically, both the ambient temperature and the intermediate temperature, with each of the two cycles being oppositely impacted by changes in the intermediate temperature, influence the system’s performance. In addition, the margin temperature negatively affects the performance, but its adoption is crucial to the system as it is used to satisfy the pinch constraint. However, because it has a similar COP trend, the lower CO_2 cycle has a greater impact on the system's overall performance.

Moreover, under high heating regimes (47–55°C), the proposed system performs better than the conventional system, which relies on the use of propane refrigerant; but, at lower heating regimes (30–35°C), the propane system is more advantageous. However, despite this advantage over the proposed system, the suggested one offers numerous benefits in terms of operational and environmental safety that align with today’s regulations, and thus should replace the conventional one.

Overall, the findings show that this system is a viable and sustainable substitute for domestic hot water production and residential heating applications, especially in situations that require higher temperature regimes. Therefore, this system can be considered for implementation in residential buildings.

References

[1] « Annual Energy Outlook 2023 U.S. Energy Information Administration », U.S. Energy Information Administration, mars 2023.

[2] « Net Zero Strategy: Build Back Greener », HM Government, oct. 2021.

[3] J. Brozovsky, A. Gustavsen, et N. Gaitani, « Zero emission neighbourhoods and positive energy districts – A state-of-the-art review », *Sustain. Cities Soc.*, vol. 72, p. 103013, sept. 2021, doi: 10.1016/j.scs.2021.103013.

[4] « DIRECTIVE OF THE EUROPEAN PARLIAMENT AND OF THE COUNCIL », Brussels, juill. 2021.

[5] M. Arnaudo, J. Dalgren, M. Topel, et B. Laumert, « Waste heat recovery in low temperature networks versus domestic heat pumps - A techno-economic and environmental analysis », *Energy*, vol. 219, p. 119675, mars 2021, doi: 10.1016/j.energy.2020.119675.

[6] Q. Tu, L. Zhang, X. Yuan, J. Jiang, et C. Deng, « Comparative performance and injection characteristic of air source heat pump with conventional and active refrigerant injection », *Case Stud. Therm. Eng.*, vol. 53, p. 103775, janv. 2024, doi: 10.1016/j.csite.2023.103775.

[7] Z. Ding, W. Wu, Y. Chen, et Y. Li, « Dynamic simulation and parametric study of solar water heating system with phase change materials in different climate zones », *Sol. Energy*, vol. 205, p. 399-408, juill. 2020, doi: 10.1016/j.solener.2020.05.075.

[8] K. Lygnerud, J. Ottosson, J. Kensby, et L. Johansson, « Business models combining heat pumps and district heating in buildings generate cost and emission savings », *Energy*, vol. 234, p. 121202, nov. 2021, doi: 10.1016/j.energy.2021.121202.

[9] V. Spasic, « Another record year for European heat pump market – sales soar 38% », févr. 2023.

[10] D. Wu et B. Hu, « Performance analysis of water refrigerant heat pump with different configurations for high-temperature application », *Front. Energy Res.*, vol. 11, p. 1257865, nov. 2023, doi: 10.3389/fenrg.2023.1257865.

[11] B. T. Austin et K. Sumathy, « Transcritical carbon dioxide heat pump systems: A review », *Renew. Sustain. Energy Rev.*, vol. 15, nº 8, p. 4013-4029, oct. 2011, doi: 10.1016/j.rser.2011.07.021.

[12] W. Wu et H. M. Skye, « Progress in ground-source heat pumps using natural refrigerants », *Int. J. Refrig.*, vol. 92, p. 70-85, août 2018, doi: 10.1016/j.ijrefrig.2018.05.028.

[13] C. Baek, J. Heo, J. Jung, H. Cho, et Y. Kim, « Optimal control of the gas-cooler pressure of a CO2 heat pump using EEV opening and outdoor fan speed in the cooling mode », *Int. J. Refrig.*, vol. 36, nº 4, p. 1276-1284, juin 2013, doi: 10.1016/j.ijrefrig.2013.02.009.

[14] P. Nekså, H. Rekstad, G. R. Zakeri, et P. A. Schiefloe, « CO2-heat pump water heater: characteristics, system design and experimental results », *Int. J. Refrig.*, vol. 21, nº 3, p. 172-179, mai 1998, doi: 10.1016/S0140-7007(98)00017-6.

[15] N. Calabrese, R. Mastrullo, A. W. Mauro, P. Rovella, et M. Tammaro, « Performance analysis of a rooftop, air-to-air heat pump working with CO 2 », *Appl. Therm. Eng.*, vol. 75, p. 1046-1054, janv. 2015, doi: 10.1016/j.applthermaleng.2014.10.057.

[16] M. N. Šarevski et V. N. Šarevski, « Characteristics of R718 refrigeration/heat pump systems with two-phase ejectors », *Int. J. Refrig.*, vol. 70, p. 13-32, oct. 2016, doi: 10.1016/j.ijrefrig.2016.07.007.

[17] R. Wang, H. Yan, D. Wu, J. Jiang, et Y. Dong, « High temperature heat pumps for industrial heating processes using water as refrigerant », *Energy*, vol. 313, p. 133847, déc. 2024, doi: 10.1016/j.energy.2024.133847.

[18] A. Zini, L. Socci, G. Vaccaro, A. Rocchetti, et L. Talluri, « Working Fluid Selection for High-Temperature Heat Pumps: A Comprehensive Evaluation », *Energies*, vol. 17, nº 7, p. 1556, mars 2024, doi: 10.3390/en17071556.

[19] B. Dai *et al.*, « Life cycle performance evaluation of cascade-heating high temperature heat pump system for waste heat utilization: Energy consumption, emissions and financial analyses », *Energy*, vol. 261, p. 125314, déc. 2022, doi: 10.1016/j.energy.2022.125314.

[20] nPro, « Load profiles for residential buildings ». [En ligne]. Disponible sur: https://www.npro.energy/main/en/load-profiles/residential

[21] L. Nolting, S. Steiger, et A. Praktiknjo, « Assessing the validity of European labels for energy efficiency of heat pumps », *J. Build. Eng.*, vol. 18, p. 476-486, juill. 2018, doi: 10.1016/j.jobe.2018.02.013.

[22] R. Llopis, L. Nebot-Andrés, R. Cabello, D. Sánchez, et J. Catalán-Gil, « Experimental evaluation of a CO2 transcritical refrigeration plant with dedicated mechanical subcooling », *Int. J. Refrig.*, vol. 69, p. 361-368, sept. 2016, doi: 10.1016/j.ijrefrig.2016.06.009.